First-principles study of $TiB_2$(0001) surfaces



2006 J. Phys.: Condens. Matter 18 4197

(http://iopscience.iop.org/0953-8984/18/17/008)

INSTITUTE OF PHYSICS PUBLISHING JOURNAL OF PHYSICS: CONDENSED MATTER

J. Phys.: Condens. Matter **18** (2006) 4197–4205 doi:10.1088/0953-8984/18/17/008

# First-principles study of $TiB_2(0001)$ surfaces

**Yanfeng Han, Yongbing Dai, Da Shu, Jun Wang and Baode Sun**

State Key Laboratory of Metal Matrix Composites, Shanghai Jiao Tong University, 1954 Huashan Road, Shanghai 200030, People's Republic of China

E-mail: yfhan@sjtu.edu.cn and bdsun@sjtu.edu.cn

Received 4 September 2005
Published 13 April 2006
Online at stacks.iop.org/JPhysCM/18/4197

**Abstract**

The $TiB_2(0001)$ surfaces are calculated using the first-principles total-energy plane-wave pseudopotential method based on density functional theory. It is found that there are large relaxations within the top three layers for both termination surfaces, and the outermost and second interlayer relaxations for B-terminated surfaces are much larger than those for Ti-terminated surfaces. The charge depletion in the vacuum and the charge accumulations in the interlayer region between the first and second layers reinforces the interlayer Ti–B chemical bonds and reduces the outermost interlayer distance. Simultaneously, the charge accumulation for B-terminated surface is more than that for Ti-terminated surface, and the interlayer Ti–B bonds between the second and third layers are weakened more for the B-terminated surface. The Ti-terminated surface is thermodynamically more favourable in most of the range of $\mu_B^{slab}$.

## 1. Introduction

The $AlB_2$-type transition-metal diborides (TMDBs), which have a stacking of intercalated graphite-like boron sheets and hexagonal layers of the metals, possess many unexpected properties and have recently been investigated extensively in many aspects. In particular, as one of the $AlB_2$-type TMDBs, $TiB_2$ possesses many unique physical properties, such as high melting point, hardness, chemical stability, high thermal conductivity, low electrical resistivity, and low work function [1]. The application of $TiB_2$ includes *in situ* particulate-reinforced composites [2, 3], grain refiner [4], light-weight high-temperature structural materials, impact resistant armor, cutting tools, wear resistant coatings [5, 6], and so on.

Many papers on the structure and properties of bulk TMDBs have been published. It is reported that the bonding in TMDBs is a combination of ionic, covalent and metallic nature and can be explained by a combination of the $sp^2$ hybrid state and the $p_z$ state of the boron network and the d and s states of the transition metals (TMs) [7–9]. The TM–B interaction also plays an important role in the bonding of TMDBs [10, 11]. There are two conflicting opinions regarding electron transfer between the B and TM atoms, which is closely related to

the chemical bonding between the TM and boron layers. However, much recent research has revealed that charge transfer from the TM to the boron atoms is evident [12–14].

In addition to many studies on the bulk properties of TMDBs, the study of TMDB surfaces has recently become more and more attractive. The structure and electronic properties of $TaB_2(0001)$ [15–17], $HfB_2(0001)$ [18], $ZrB_2(0001)$ [19], $WB_2(0001)$ [20] and $NbB_2(0001)$ [19] surfaces have been investigated experimentally. It is found that the group-IV (Zr, Hf)$B_2(0001)$ and group-V (Ta, Nb)$B_2(0001)$ surfaces are terminated with the metal layer and boron layer, respectively, and the surface core-level shift was particularly emphasized. At the same time, the self-consistent-charge discrete variational-X$\alpha$ calculations of $TaB_2(0001)$ surfaces and the first-principles calculations of (Ta, Nb)$B_2(0001)$ [16, 19, 21] and (Zr, Hf)$B_2(0001)$ [19, 21, 22] surfaces have also been performed. It was reported that the (Zr, Hf)-terminated (Zr, Hf)$B_2(0001)$ surface and the B-terminated (Ta, Nb)$B_2(0001)$ surface are likely to be stable, which is in accordance with experimental results. To our knowledge, no experimental studies on $TiB_2(0001)$ surfaces have been reported so far, because high-grade $TiB_2$ crystals are not easily obtained, and also no theoretical research is available. However, the characteristics of $TiB_2$ surfaces are not only basic scientific concerns but also important for engineering applications, especially in composites [2, 3] and grain refiner [4]. Within such applications, the crystal structure and the electronic properties of the $TiB_2$ surface, e.g., the preferred atomic species of the termination layer, may significantly influence the combination between the $TiB_2$ particles and the metal matrix. In addition, study of the $TiB_2$ surface can provide primitive information about the substrate for the epitaxial growth of aluminium on the $TiB_2$ surface, which is helpful for understanding the possible nucleation mechanism of aluminium on it.

In this paper, using the first-principles total-energy plane-wave pseudopotential method based on density functional theory (DFT), we have investigated the $TiB_2(0001)$ surfaces, focusing on their structure and properties.

## 2. Computational details and surface geometry

The calculations in the present paper were performed using special point integration over the Brillouin zone [23, 24] and a plane-wave basis set for the expansion of the wave functions [25, 26]. The minimum total energy of the structure is achieved by relaxing automatically the internal coordinates using the Broyden–Fletcher–Goldfarb–Shanno (BFGS) algorithm [27]. The atomic configurations of Ti and B generated from the ultrasoft pseudopotential that was used were $3s^2 3p^6 3d^2 4s^2$ and $2s^2 2p^1$, respectively [28]. The generalized gradient approximation (GGA) of Perdew *et al* was used to treat the exchange interactions and correlation effects [29]. A plane-wave cutoff energy of 380 eV was employed in the calculations, which assured a total energy convergence of $10^{-6}$ eV/atom. Brillouin zone sampling was performed using $10\times10\times8$ and $10\times10\times1$ Monkhorst–Pack $k$-points meshes for bulk and surface calculations, respectively. The Mulliken charge population was also calculated according to the formalism described by Segall *et al* [30, 31].

The crystal structure of bulk $TiB_2$ is $AlB_2$-type with the space group symmetry $P6/mmm$, which is designated $C32$. It adopts a layered hexagonal structure with alternating closed-packed hexagonal layers of titanium and graphite-like boron layers. The equilibrium lattice constants attained by bulk calculations are $a = 3.0292$ Å and $c = 3.2196$ Å ($c/a = 1.063$), which are in satisfactory agreement with the experimental and other calculation results of $a = 3.026$ Å and $c = 3.228$ Å ($c/a = 1.067$) [9], $a = 3.028$ Å and $c = 3.228$ Å ($c/a = 1.066$) [10], and $a = 3.070$ Å and $c = 3.262$ Å ($c/a = 1.063$) [12]. The following surface optimizations are all based on this bulk geometry. In the surface calculations, to eliminate spurious dipole

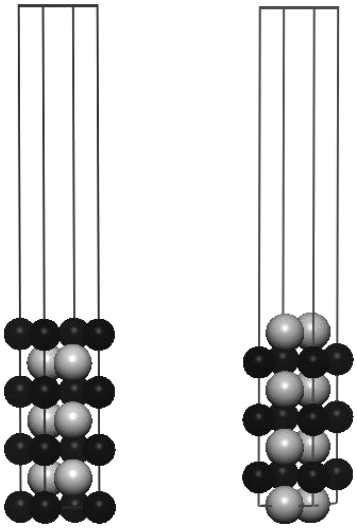


**Figure 1.** Schematic diagrams of Type I (a) and Type II (b) slabs with seven layers. The dark spheres represent Ti atoms; the gray spheres represent B atom.

effects, symmetric slabs were used, since the polar $TiB_2(0001)$ surface is terminated with only one species of Ti or B atom. Repeated Ti-terminated ($1 \times 1$) slabs (denoted Type I) and B-terminated ($1 \times 1$) slabs (denoted Type II) with 3, 5, 7, 9, 11 layers were employed. To prevent interactions between periodic images, a 20 Å vacuum region was added in all the supercell geometries. Type I and Type II slabs with seven layers are shown schematically in figure 1. All the atoms in the slabs were relaxed to a force tolerance of 0.03 eV $Å^{-1}$.

## 3. Results and discussions

### *3.1. Structural relaxations*

Surface reconstruction does not happen for both termination surfaces after full relaxation. Table 1 lists the results of $TiB_2(0001)$ surface relaxations as a function of termination and slab thickness. From the table, it is shown that the expansion/contraction effect does not happen on moving into deeper layers in both termination surfaces. Relaxations for both termination surfaces are all large, and the effects of relaxation are mainly localized within the top three atomic layers. When the slab thickness, $n$, is more than seven, the top three interlayer relaxations for both termination surfaces are all well converged, which implies that the slabs with more than seven atomic layers possess a bulk-like interior. Therefore, the remaining results are based on the slab with nine atomic layers. The results in the table also demonstrate that the outermost and second interlayer relaxations for Type II surfaces are much larger than those for Type I surfaces in all the slabs. It is observed that the outermost interlayer distances of Type I and II surfaces with nine atomic layers are reduced by 4.8% and 7.0% of those in the bulk, respectively, and the second interlayer distances are enlarged by 0.8% and 2.4%, respectively. Thus, the Type I surfaces are likely to be more stable than Type II surfaces. The stability difference for both termination surfaces and the large amplitude of surface relaxation may be useful information for further study of the adhesion between $TiB_2$ and the metal matrix and the possible nucleation of aluminium on $TiB_2$. However, it is a pity

**Table 1.** $TiB_2(0001)$ surface relaxations as a function of termination and slab thickness (change of the interlayer spacing $\Delta_{ij}$ as a percentage of the spacing in the bulk).

| | | Slab thickness, $n$ | | | | |
|---|---|---|---|---|---|---|
| Termination | Interlayer | 3 | 5 | 7 | 9 | 11 |
| Ti | $\Delta_{12}$ | −3.8 | −4.5 | −4.7 | −4.8 | −4.7 |
| | $\Delta_{23}$ | | 0.9 | 0.4 | 0.8 | 0.7 |
| | $\Delta_{34}$ | | | 0.53 | 0.3 | 0.4 |
| | $\Delta_{45}$ | | | | −0.2 | 0.3 |
| | $\Delta_{56}$ | | | | | −0.4 |
| B | $\Delta_{12}$ | −5.4 | −7.7 | −7.0 | −7.0 | −7.0 |
| | $\Delta_{23}$ | | 2.8 | 2.2 | 2.4 | 2.3 |
| | $\Delta_{34}$ | | | 0 | 0.2 | 0.1 |
| | $\Delta_{45}$ | | | | −0.6 | −0.2 |
| | $\Delta_{56}$ | | | | | −0.4 |

**Table 2.** Effective atomic charges for Type I and II $TiB_2(0001)$ surfaces.

| | | | Charge (electron) | |
|---|---|---|---|---|
| Termination | Layer number | Species | Relaxed | Unrelaxed |
| Ti | 1 | Ti | 0.52 | 0.49 |
| | 2 | B | −0.57 | −0.56 |
| | 3 | Ti | 1.19 | 1.20 |
| | 4 | B | −0.58 | −0.58 |
| | 5 | Ti | 1.18 | 1.17 |
| B | 1 | B | −0.44 | −0.40 |
| | 2 | Ti | 1.45 | 1.39 |
| | 3 | B | −0.58 | −0.59 |
| | 4 | Ti | 1.17 | 1.16 |
| | 5 | B | −0.58 | −0.58 |

that there are no any experimental and theoretical data for $TiB_2(0001)$ surfaces in the existing publications with which to compare these results. These results are similar to those in other calculations of $ZrB_2$ and $HfB_2$ of the same group TMDB [19, 21] and therefore our calculation seems to be reasonable. However, only a Zr-terminated surface with 13 layers was investigated in the $ZrB_2$ calculations. In the $HfB_2$ calculations, a slab with seven layers was employed and the considerations of surface relaxation were restricted to only the outermost and second interlayers. As for $TaB_2$ and $NbB_2$ (two group-V TMDBs), in contrast to $TiB_2$ and other group-IV TMDBs ($ZrB_2$ and $HfB_2$), the B-terminated (0001) surfaces exhibit smaller relaxation than the TM-terminated surfaces, i.e., B-terminated surfaces are likely to be more stable [19, 21].

### *3.2. Electronic structure of $TiB_2(0001)$ surface*

The calculated effective atomic charges for Types I and II $TiB_2(0001)$ ideal and relaxed surfaces using the Mulliken population analysis are given in table 2. It is found that the effective atomic charges for the atoms from the upper layers to the inner layers differ slightly after full relaxation, which implies that the charge transfers from the Ti layer to the B layer between the top two layers for both termination surfaces are small. Thus, it is impossible for the small charge transfers to strengthen the chemical bonds between B atoms in the first or second

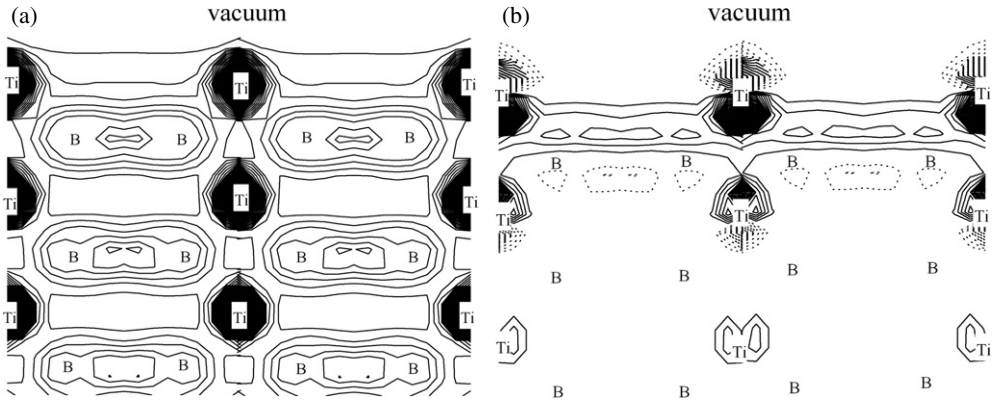


**Figure 2.** Distribution of charge density (a) and difference in charge density (relative to the ideal surface) (b) on the $(11\bar{2}0)$ plane for the Type I $TiB_2$ surface after full relaxation. The contours are from 0.000 156 $au^{-3}$ to 9.5504 $au^{-3}$ in spacing of 0.1 $au^{-3}$ in figure (a). Solid and dotted lines indicate positive and negative values, respectively, in figure (b).

layer for both termination surfaces. The calculated B–B bond lengths in the second or first layer for Types I and II surfaces are 1.747 and 1.743 Å, respectively, which are close to the bond length in the ideal surfaces, 1.748 Å. Accordingly, the lateral lattice structures of both termination surfaces are trivially affected after full relaxation. These charge transfers among the atomic layers in the $TiB_2$ surface are similar to the calculation results of the $HfB_2$ surface [21]. However, the calculated effective atomic charges for the $HfB_2$ surface were not presented. It should be noticed that charge transfer is related to the valence of TMs, e.g., for the B-terminated (0001) $TaB_2$ surface, since Ta has one more valence electron than group-IV TMs, the transferred charge from the second Ta layer to the first B layer is large enough to strengthen B–B bonds and, simultaneously, the bonds between the first and second layers are weakened [16, 21], which is contrary to the Type II surface in this paper. The difference in transferred charge may partially be the reason why the favourable types of termination surfaces are different for group-IV and group-V TMDBs.

To further analyze the electronic structures of the surfaces, the distributions of valence charge density of relaxed surfaces and the differences between the charge densities of the relaxed and unrelaxed surfaces on the $(11\bar{2}0)$ plane for Types I and II $TiB_2(0001)$ surfaces are shown in figures 2 and 3, respectively. From the distributions of charge density of Types I and II surfaces shown in figures 2(a) and 3(a), it can be seen that strong covalent B–B bonds exist between B atoms in the same layer and that Ti–B bonds form between the neighbouring layers, which has been observed in theoretical and experimental works on bulk $TiB_2$ [10, 12, 13]. As shown in figures 2(b) and 3(b), the relaxations only influence the top three layers for both termination surfaces. Charge depletion happens in the vacuum and there are charge accumulations in the interlayer region between the first and second layers after full relaxation for both termination surfaces. Thus, the interlayer Ti–B chemical bonds are reinforced and the outermost interlayer distances are largely reduced, as can be found in table 1. It is also evident that charge accumulation in the interlayer region between the first and second layers for Type II surfaces is more than that for Type I surfaces after full relaxation. Consequently, the outermost interlayer relaxation for Type II surfaces is much larger than that for Type I surfaces, which has also been shown in table 1. The charge depletion and accumulation occur simultaneously between the second and third layers for the Type I surface. However, only charge depletion

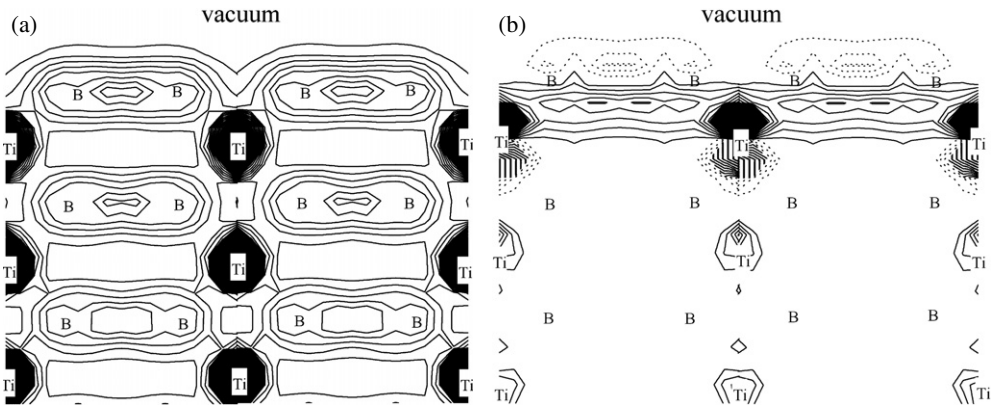


**Figure 3.** Distribution of charge density (a) and difference in charge density (relative to the ideal surface) (b) on the $(11\bar{2}0)$ plane for the Type II $TiB_2(0001)$ surface after full relaxation. The contours are from 0 $au^{-3}$ to 9.5375 $au^{-3}$ in spacing of 0.1 $au^{-3}$ in figure (a). Solid and dotted lines indicate positive and negative values, respectively, in (b).

exists in the corresponding region for the Type II surface. Therefore, as shown in table 1, the interlayer distance between the second and third layers for the Type II surface expands more than that for the Type I surface, which results in greater weakening of bonds between the second and third layers for the Type II surface. The charge density difference after full relaxation for Hf-terminated $HfB_2$ surfaces, as the same group TMDB, has been reported [21], and the calculation results are trivially different to the results in this paper. However, investigations of the charge density difference of $HfB_2$ surfaces are only limited to the Hf-terminated surface and the outermost interlayer region between the first Hf and the second B layers. But our results show that the charge density difference in the region between the second and the third layers is not negligible and should be taken into account to understand the relaxation behaviour of the $TiB_2$ surface.

### *3.3. Stabilities of $TiB_2(0001)$ surfaces*

The stabilities of Types I and II surfaces are also compared in terms of the surface energy. Since symmetric slabs are employed in the surface calculations, the supercells in the present calculations are non-stoichiometric slabs. The chemical potentials of the Ti and B atoms should be taken into consideration when calculating the surface energies of $TiB_2(0001)$ surfaces. The surface energy ($\sigma$) can be defined as [32, 33]:

$$\sigma = \frac{1}{2A}(E_{\text{slab}} - N_{\text{Ti}}\mu_{\text{Ti}}^{\text{slab}} - N_{\text{B}}\mu_{\text{B}}^{\text{slab}} + PV - TS) \tag{1}$$

where $A$ is the surface area, $E_{\text{slab}}$ is the total energy of a fully relaxed nine-layer Type I or Type II supercell, $N_{\text{B}}$ and $N_{\text{Ti}}$ are the numbers of the B and Ti atoms in the supercell, respectively, and $\mu_{\text{B}}^{\text{slab}}$ and $\mu_{\text{Ti}}^{\text{slab}}$ are the chemical potentials of B and Ti in the slab, respectively. $P$, $V$, $T$ and $S$ denote the pressure, volume, temperature and entropy of the system, respectively. The terms $PV$ and $TS$ can be neglected at 0 K and typical pressures. In the calculations, it is also assumed that the surface is in equilibrium with the bulk. Thus, the chemical potential of the bulk $TiB_2$ ($\mu_{\text{TiB}_2}^{\text{bulk}}$) is expressed by:

$$\mu_{\text{TiB}_2}^{\text{bulk}} = \mu_{\text{Ti}}^{\text{slab}} + 2\mu_{\text{B}}^{\text{slab}}. \tag{2}$$

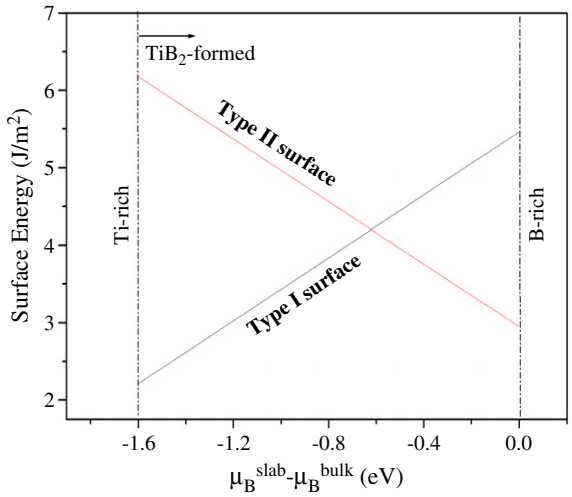


**Figure 4.** Surface energy for the $TiB_2$(0001) surface as a function of the chemical potential of B. (This figure is in colour only in the electronic version)

Thus, equation (1) can be rewritten in terms of $\mu_B^{slab}$:

$$\sigma = \frac{1}{2A}(E_{slab} - N_{Ti}\mu_{TiB_2}^{bulk} + \mu_B^{slab}(2N_{Ti} - N_B)). \tag{3}$$

Moreover, the chemical potential of the bulk $TiB_2$ ($\mu_{TiB_2}^{bulk}$) is related to its 0 K heat of formation ($\Delta H_f^0$) and the chemical potentials of Ti and B in their bulk phase ($\mu_{Ti}^{bulk}$ and $\mu_B^{bulk}$) are shown as:

$$\mu_{TiB_2}^{bulk} = \mu_{Ti}^{bulk} + 2\mu_B^{bulk} + \Delta H_f^0. \tag{4}$$

Combining equation (2) with (4), the following relation can be given:

$$\mu_B^{slab} - \mu_B^{bulk} = \tfrac{1}{2}(\Delta H_f^0 + \mu_{Ti}^{bulk} - \mu_{Ti}^{slab}). \tag{5}$$

Additionally, the chemical potentials of Ti and B in the slab must be less than those in their bulk phases, respectively. Otherwise, the compound slab would be unstable and form the more favourable elemental bulk phases energetically. Therefore, the range of the B chemical potential thermodynamically is:

$$\tfrac{1}{2}\Delta H_f^0 \leqslant \mu_B^{slab} - \mu_B^{bulk} \leqslant 0. \tag{6}$$

The calculation of $\mu_B^{bulk}$ was performed on bulk $\alpha$-$B_{12}$. The calculation result of $\Delta H_f^0$ is $-3.2$ eV, which is in good agreement with the experimental value of $-3.4$ eV [34].

The surface energies for Type I and II $TiB_2$(0001) surfaces as a function of the B chemical potential ($\mu_B^{slab} - \mu_B^{bulk}$) are shown in figure 4. It is found that the Type I surface is more stable than the Type II surface at low B chemical potential, $\mu_B^{slab} - \mu_B^{bulk}$. The surface energy of the Type II surface is reduced and the surface energy of the Type I surface is raised with increasing B chemical potential $\mu_B^{slab} - \mu_B^{bulk}$. Therefore, the Type II surface becomes more stable at high B chemical potential. However, the Type I (0001) surface is thermodynamically more favourable over most of the range of $\mu_B^{slab}$, which needs to be proved by further experimental study. Therefore, the relative stabilities of both termination surfaces should be taken into account in further research on the interface between $TiB_2$ and the metal matrix. Meanwhile, the surface energies for both termination surfaces are all large, which indicates the reactive features of both

termination surfaces. The surface stability of $TiB_2$ in our calculation is similar to that of $ZrB_2$ and $HfB_2$, as the same group TMDBs, in other calculations and experiment [19, 21, 22]. Thus, it is likely to be a common law for the group-IV TMDBs that the transition-metal termination surface is more stable than the B-terminated surface from the viewpoint of crystal structure and surface energy.

## 4. Conclusions

We have calculated the Ti- and B-terminated $TiB_2(0001)$ surfaces using the first-principles total-energy plane-wave pseudopotential method based on density functional theory. The effects of relaxation are mainly localized within the top three atomic layers for both termination surfaces and the outermost and second interlayer relaxations for B-terminated surfaces are much larger than those for Ti-terminated surfaces in all the slabs. Charge depletion in the vacuum and charge accumulations in the interlayer region between the first and second layers after full relaxation for Ti- and B-terminated surfaces reinforce the interlayer Ti–B chemical bonds and reduce the outermost interlayer distances. The larger charge accumulation in the interlayer region between the first and second layers results in larger outermost interlayer relaxation for the B-terminated surface than that for the Ti-terminated surface. The coexisting charge depletion and accumulation between the second and third layers for the Ti-terminated surface brings about less weakening of bonds between the second and third layers for the Ti-terminated surface than for the B-terminated surface. The charges slightly transfer from the Ti layer to the B layer between the top two layers for both termination surfaces. The surface energies for both termination surfaces are all large, and the Ti-terminated (0001) surface is thermodynamically more favourable over most of the range of $\mu_B^{slab}$. It is likely to be a common law for the group-IV TMDBs that the transition-metal termination surface is more stable than the B-terminated surface.

## Acknowledgments

The authors gratefully thank financial support from the High Technology Research and Development Program of China (No 2002AA336072), the Program of Shanghai Subject Chief Scientist (No 03XD14009) and the Nanotechnology Foundation of Shanghai (No 0452nm058). The authors also truly appreciate the anonymous referees' insightful suggestions, which led to improvements in the paper.

## References

[1] Gordon W and Soffer S B 1975 *J. Phys. Chem. Solids* **36** 627
[2] Bartels C, Raabe D and Gottstein G 1997 *Mater. Sci. Eng.* A **237** 12
[3] Lloyd D J 1994 *Int. Mater. Rev.* **39** 1
[4] Greer A L, Bunn A M, Tronche A, Evans P V and Bristow D J 2000 *Acta Mater.* **48** 2823
[5] Munro R G 2000 *J. Res. Natl Inst. Stand. Technol.* **105** 709
[6] Loundquist B, Myers H and Westin R 1960 *Phil. Mag.* **33** 1187
[7] Perkins P G and Sweeney A V J 1976 *J. Less-Common Met.* **47** 165
[8] Ihara H, Hirabayashi M and Nakagawa H 1977 *Phys. Rev.* B **16** 726
[9] Burdett J K, Canadell E and Miller G J 1986 *J. Am. Chem. Soc.* **108** 6561
[10] Tian D C and Wang X B 1992 *J. Phys.: Condens. Matter* **4** 8765
[11] Wang X B, Tian D C and Wang L L 1994 *J. Phys.: Condens. Matter* **6** 10185
[12] Vajeeston P, Ravindran P, Ravi C and Asokamani R 2001 *Phys. Rev.* B **63** 045115
[13] Lie K, Brydson R and Davock H 1999 *Phys. Rev.* B **59** 5361

[14] Lie K, Høier R and Brydson R 2000 *Phys. Rev.* B **61** 1786
[15] Kawanowa H, Souda R, Otani S and Gotoh Y 1998 *Phys. Rev. Lett.* **81** 2264
[16] Kawanowa H, Souda R, Yamamoto K, Otani S and Gotoh Y 1999 *Phys. Rev.* B **60** 2855
[17] Perkins C L, Singh R, Trenary M, Tanaka T and Paderno Y 2001 *Surf. Sci.* **470** 215
[18] Hayami W, Souda R, Aizawa T and Tanaka T 1998 *Surf. Sci.* **415** 433
[19] Aizawa T, Suehara S, Hishita S, Otani S and Arai M 2005 *Phys. Rev.* B **71** 165405
[20] Kawanowa H, Gotoh Y, Otani S, Yamamoto K and Souda R 2000 *Surf. Sci.* **454–456** 49
[21] Yamamoto K, Kobayashi K, Kawanowa H and Souda R 1999 *Phys. Rev.* B **60** 15617
[22] Hayami W, Aizawa T, Tanaka T and Otani S 2004 *J. Phys. Chem.* B **108** 15233
[23] Payne M C, Teter M P, Allan D C, Arias T A and Joannopoulos J D 1992 *Rev. Mod. Phys.* **64** 1045
[24] Segall M D, Lindan P J D, Probert M J, Pickard C J, Hasnip P J, Clark S J and Payne M C 2002 *J. Phys.: Condens. Matter* **14** 2717
[25] Hohenberg P and Kohn W 1964 *Phys. Rev.* B **136** 864
[26] Monkhorst H J and Pack J D 1977 *Phys. Rev.* B **16** 1748
[27] Fischer T H and Almlof J 1992 *J. Phys. Chem.* **96** 9768
[28] Vanderbilt D 1990 *Phys. Rev.* B **41** 7892
[29] Perdew J P, Burke K and Ernzerhof M 1996 *Phys. Rev. Lett.* **77** 3865
[30] Segall M D, Pickard C J, Shah R and Payne M C 1996 *Mol. Phys.* **89** 571
[31] Segall M D, Pickard C J, Shah R and Payne M C 1996 *Phys. Rev.* B **54** 16317
[32] Rapcewicz K, Chen B, Yakobson B and Bernhole J 1998 *Phys. Rev.* B **57** 7281
[33] Batyrev I, Alavi A and Finnis M W 2000 *Faraday Discuss.* **114** 33
[34] Topor L and Kleppa O J 1985 *J. Chem. Thermodyn.* **17** 1003